

Mechanistic Studies of Pd(II)-Catalyzed Copolymerization of Ethylene and Vinylalkoxysilanes: Evidence for a β -Silyl Elimination Chain Transfer Mechanism

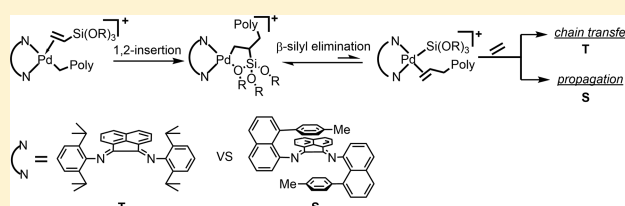
Zhou Chen,[†] Weijun Liu,^{‡,§} Olafs Daugulis,^{*,†} and Maurice Brookhart^{*,†,‡}

[†]Center for Polymer Chemistry, Department of Chemistry, University of Houston, Houston, Texas 77204-5003, United States

[‡]Department of Chemistry, University of North Carolina at Chapel Hill, Chapel Hill, North Carolina 27599-3290, United States

S Supporting Information

ABSTRACT: Copolymerizations of ethylene with vinyltrialkoxysilanes are reported using both a “traditional” cationic Pd(II) aryldiimine catalyst, **t-1** (aryl = 2,6-diisopropylphenyl), and a “sandwich-type” aryldiimine catalyst, **s-2** (aryl = 8-tolynaphthyl). Incorporation levels of vinyltrialkoxysilanes between 0.25 and 2.0 mol % were achieved with remarkably little rate retardation relative to ethylene homopolymerizations. In the case of the traditional catalyst system, molecular weights decrease as the level of comonomer increases and only one trialkoxysilyl group is incorporated per chain. Molecular weight distributions of ca. 2 are observed. For the sandwich catalyst, higher molecular weights are observed with many more trialkoxysilyl groups incorporated per chain. Polymers with molecular weight distributions of ca. 1.2–1.4 are obtained. Detailed NMR mechanistic studies have revealed the formation of intermediate π -complexes of the type (diimine)Pd(alkyl)-(vinyltrialkoxysilane)⁺. 1,2-Migratory insertions of these complexes occur with rates similar to ethylene insertion and result in formation of observable five-membered chelate intermediates. These chelates are rapidly opened with ethylene forming alkyl ethylene complexes, a requirement for chain growth. An unusual β -silyl elimination mechanism was shown to be responsible for chain transfer and formation of low molecular weight copolymers in the traditional catalyst system, **t-1**. This chain transfer process is retarded in the sandwich system. Relative binding affinities of ethylene and vinyltrialkoxysilanes to the cationic palladium center have been determined. The quantitative mechanistic studies reported fully explain the features of the bulk polymerization results.



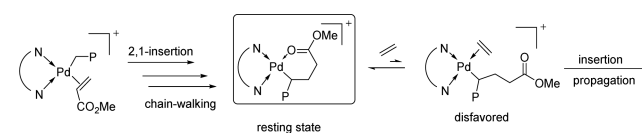
INTRODUCTION

Coordination–insertion copolymerization of olefins with polar vinyl monomers potentially offers a powerful method for the controlled, low cost synthesis of high-value functionalized polyolefins.¹ Although early transition-metal catalysts are extensively used for the coordination polymerization of nonpolar olefins such as ethylene and propylene, the use of these catalysts for copolymerization with polar vinyl monomers is limited due to their high oxophilicity.² In contrast, late transition metal catalysts display enhanced tolerance toward heteroatoms³ and can copolymerize ethylene with a range of polar vinyl monomers, such as methyl acrylate,⁴ vinyl acetate,⁵ acrylonitrile,⁶ and other common polar monomers.⁷ An early example from our group showed that cationic α -diimine Pd(II) complexes can copolymerize ethylene (and higher α -olefins) with methyl acrylate (MA) to form highly branched copolymers.^{4a,8} Neutral phosphine-sulfonate Pd(II) “Drent-type” catalysts copolymerize ethylene and MA to produce linear functionalized copolymers.⁹ A variety of other Drent-type catalysts have been used for copolymerization of several polar monomers with ethylene.^{9,10}

Copolymerizations of polar vinyl monomers with ethylene generally exhibit much lower activities relative to those of

ethylene homopolymerization.^{9–11} Various factors responsible for reduced activities have been enumerated.¹² As an example, mechanistic studies of the cationic α -diimine Pd(II) system for MA/ethylene copolymerization revealed that after 2,1 insertion of MA and rapid chain-walking, a six-membered carbonyl chelate intermediate is formed. This chelate is the catalyst resting state which is stable and strongly favored over the “chelate opened” ethylene complex required for further propagation (Scheme 1).⁸ The development of catalysts for copolymerization of ethylene with polar vinyl monomers which exhibit commercially viable activities and molecular weights remains a challenge for the field.

Scheme 1. Proposed Mechanism of α -Diimine Pd(II) Catalyzed Copolymerization of Ethylene and MA



Received: October 5, 2016

Published: December 1, 2016

Polyethylene (PE) that is functionalized with trialkoxysilane ($-\text{Si}(\text{OR})_3$) groups can be cross-linked to form PEX-b, a tough material that is widely used for coating wires and cables and in manufacturing plastic piping.¹³ The cross-links are formed by exposing the PE containing $-\text{Si}(\text{OR})_3$ groups to steam to form $-\text{Si}-\text{O}-\text{Si}-$ bridges. The $-\text{Si}(\text{OR})_3$ groups are introduced into PE either through postpolymerization radical grafting of vinylalkoxysilanes ($\text{CH}_2=\text{CHSi}(\text{OR})_3$) to PE or through radical-initiated copolymerization of ethylene with vinylalkoxysilanes.¹⁴ Vinylalkoxysilanes are polar monomers that have generally received little attention with respect to coordination–insertion polymerization using late transition metals.^{15,16} Successful copolymerizations of ethylene with vinylalkoxysilanes using α -diimine Ni(II) and Pd(II) catalysts have been reported by researchers at DuPont.¹⁷ A very significant feature of these copolymerizations is that the copolymerization activities are higher than those of the MA/ethylene copolymerizations and comparable to those of ethylene homopolymerizations. The high activities of these copolymerizations prompted us to conduct a detailed mechanistic study of the Pd-based diimine systems with the goal of understanding why these polar monomers are so effective and to assess the potential for designing even more effective catalysts.

While a number variations of aryl-substituted α -diimine Pd(II) catalysts have been devised and investigated,¹⁸ studies reported here are focused on the “traditional” catalyst, **t-1**, bearing ortho-isopropyl groups^{18e,19} and the “sandwich” catalyst **s-2**, incorporating 8-tolynaphthyl imine moieties (Figure 1).²⁰ The traditional diimine system **t-1** polymerizes

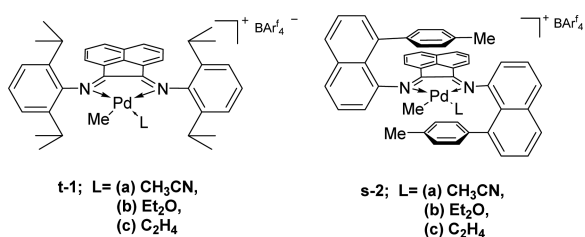


Figure 1. “Traditional” and “sandwich” Pd(II) α -diimine complexes.

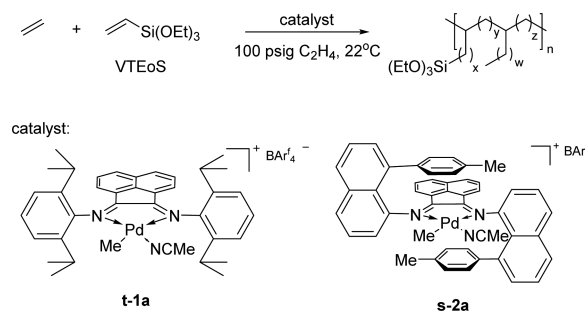
ethylene to yield hyperbranched polyethylene at 20 °C with ca. 110 branches per 1000C and M_n values in the range of 10^4 g/mol with molecular weight distributions of ca. 2.^{18e,19} The recently developed “sandwich” α -diimine catalyst **s-2** also produces hyperbranched polyethylene (ca. 110 branches/1000C) which exhibits very narrow molecular weight distributions (M_w/M_n ca. 1.1).²⁰ Comparison of associative ligand exchange rates revealed that 8-tolyl groups in **s-2** are far more effective in shielding the axial coordination sites than the ortho isopropyl groups of traditional catalyst **t-1**.²⁰ This feature results in significant reduction in the rate of chain transfer relative to the rate of propagation and thus leads to the low M_w/M_n values observed.

We present here a comprehensive account of the mechanistic details of the copolymerization of ethylene with vinylalkoxysilanes using catalysts **t-1** and **s-2**. These studies provide information regarding insertion barriers of these polar monomers, their binding affinities relative to ethylene, and the stability and properties of an intermediate chelate complex. A chain transfer mechanism involving a unique β -silyl elimination process has been identified.

RESULTS AND DISCUSSION

Copolymerization Reactions. As noted above, the catalysts employed for the copolymerization reactions are the cationic traditional isopropyl-substituted complex **t-1a** and sandwich α -diimine Pd(II) complex **s-2a** (Scheme 2). These complexes were synthesized following previously reported procedures.²⁰ Vinyltriethoxysilane (VTEoS) was chosen as a model $\text{CH}_2=\text{CHSi}(\text{OR})_3$ monomer.

Scheme 2. Copolymerization of Ethylene and VTEoS Using α -Diimine Pd(II) Complexes



The results of copolymerizations using catalyst **t-1a** are summarized in Table 1. Polymerizations were carried out in dichloromethane at 100 psig ethylene, 22 °C with varying concentrations of VTEoS. As with homopolymerization of ethylene (entry 5), the polymers obtained are highly branched with branching densities of ca. 105 branches/1000C.²¹ The mole fraction incorporation of VTEoS into the polymer is nearly proportional to the VTEoS concentration (Table 1, entries 1–3). The molecular weights of the copolymers produced are sensitive to the concentration of the VTEoS monomer. For example, complex **t-1a** produced a copolymer with M_n values of 7.0×10^3 g/mol at a VTEoS concentration of 0.52 M, 5.4×10^3 g/mol at 1.04 M VTEoS and 3.1×10^3 g/mol at 1.56 M VTEoS (entries 1–3, Table 1).²² All M_w/M_n values are ca. 2 indicating that the M_n values are chain-transfer limited. This is further verified by entry 4 where doubling the polymerization time relative to entry 1 produces a polymer with the same M_n value. Olefinic units were detected, as the polymer end groups establishing that β -elimination is responsible for chain transfer. A calculation based on mole percent incorporation and M_n values suggests that each chain contains only ca. one VTEoS unit.²³

An interesting feature, in contrast to most other ethylene/polar vinyl monomer copolymerizations,¹² is that the turnover frequency (TOF) for the copolymerizations is not dramatically reduced relative to the TOF for homopolymerization of ethylene under similar conditions. For example, compare the TOF of entry 1 (0.52 M VTEoS) of 362 h^{-1} with that of homopolymerization (entry 5) of 456 h^{-1} . The TOF drops only slightly as VTEoS concentration increases (e.g., 362 h^{-1} at 0.52 M; 227 h^{-1} at 1.04 M).²⁴

The mechanistic studies described below will clarify the mechanisms of chain transfer, the reason for one VTEoS per chain, and the near insensitivity of the TOF to VTEoS. The results of copolymerizations using sandwich catalyst **s-2a** are also summarized in Table 1. TOFs are approximately a factor of 10 lower than those observed for analogous runs using traditional catalyst **t-1a**, and this is consistent with previously observed comparisons of homopolymerizations of ethylene

Table 1. Copolymerization of Ethylene and VTEoS Using Pd(II) Catalysts

entry ^a	precatalyst	[VTEoS]	weight/g	TOF/h ⁻¹	incorp. (mol %) ^b	branches/1000C ^b	α -olefins (%) ^b	M_n ($\times 10^{-3}$ g/mol) ^c	M_w/M_n ^c
1	t-1a	0.52 M	2.23	362	0.26	106	58	7.0	2.0
2	t-1a	1.04 M	1.40	227	0.45	108	66	5.4	2.1
3	t-1a	1.56 M	1.15	187	0.71	106	72	3.1	2.3
4 ^d	t-1a	0.52 M	3.72	302	0.26	106	58	7.4	2.1
5	t-1a	0	2.81	456	n.o. ^g	109	n.d. ^h	12.1	2.4
6	s-2a	0.52 M	0.27	44	0.58	99	n.d. ^h	18.1	1.4
7	s-2a	1.04 M	0.29	47	1.30	98	n.d. ^h	17.2	1.2
8 ^e	s-2a	1.56 M	0.85	46	2.03	100	n.d. ^h	13.3	1.4
9 ^d	s-2a	0.52 M	0.41	33	0.57	97	n.d. ^h	30.7	1.3
10 ^f	s-2a	0.52 M	0.71	25	0.54	101	n.d. ^h	40.8	1.4
11	s-2a	0	0.29	47	n.o. ^g	109	n.d. ^h	21.4	1.2

^aConditions: $V(\text{total}) = 10$ mL, 10 μmol of Pd catalyst, 22 h, 100 psig ethylene, dichloromethane, 22 $^{\circ}\text{C}$. ^bDetermined by using ^1H NMR spectroscopy. The percentage (%) of α -olefin is the fraction of terminal olefin in all olefin groups. ^cMolecular weight was determined by SEC in trichlorobenzene at 140 $^{\circ}\text{C}$. ^d44 h. ^e30 μmol of Pd catalyst. ^f100 h. ^gNot observed. ^hNot determined due to high molecular weights of the polymers.

with these two catalysts.²⁰ As in the case of catalyst s-2a, highly branched polymers are produced (ca. 100 branches/1000C).²¹

Remarkably, the TOFs observed in the copolymerization runs using s-2a are nearly the same as that for the homopolymerization (compare entry 11 for the homopolymerization with entries 6 and 7). Molecular weight distributions, as in the case for ethylene homopolymerizations using this catalyst,²⁰ are narrow (ca. 1.2–1.4 under these conditions) and substantially less than 2; thus, M_n values have not reached their chain-transfer limited values. Thus, even though turnover frequencies are significantly less for catalyst s-2a versus those for catalyst t-1a, significantly higher molecular weight polymers can be generated (compare results in entries 1–4 vs 6–9). For example, the molecular weight M_n of copolymer produced in entry 10 by catalyst s-2a reached 40.8×10^3 g/mol with a narrow distribution retained ($M_w/M_n = 1.4$).

In contrast to copolymers produced by t-1a, copolymers generated by s-2a exhibit more than one VTEoS monomer per chain. For example, in entry 6, there are ca. 4 VTEoS units on average per chain while for entries 7 and 10 there are ca. 8 VTEoS monomers on average per chain. In contrast to copolymerizations using catalyst t-1a, it is clear that VTEoS does not induce rapid chain transfer. Mechanistic studies described below will illuminate the difference in behaviors of these two catalytic systems and demonstrate that β -silyl elimination is responsible for chain transfer using the traditional catalyst.

Mechanistic Studies. Low Temperature NMR Studies of Migratory Insertion Reactions of Vinyltrialkoxysilanes: Barriers and Activation Parameters. The complexes employed for mechanistic studies are the cationic α -diimine Pd(II) complexes t-1b, t'-3b, and s-2b (Figure 2), which were synthesized according to the reported procedures.²⁵

In order to generate simplified NMR spectra, vinyltrimethoxysilane (VTMoS) was used in place of VTEoS. Addition of 1 equiv of VTMoS to a CD_2Cl_2 solution of t-1b at -78 $^{\circ}\text{C}$ leads to clean formation of the η^2 -olefin complex t-

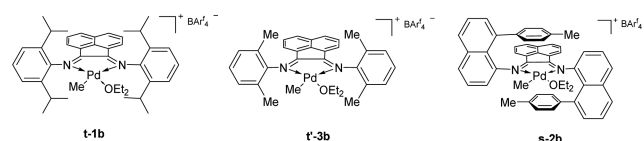
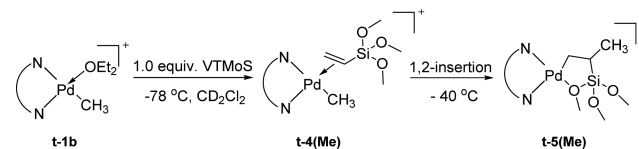


Figure 2. Cationic (α -diimine) $\text{Pd}(\text{CH}_3)(\text{OEt}_2)^+$ complexes.

4(Me) (Scheme 3). The displacement of extremely labile ether with VTMoS is fast and complete at -78 $^{\circ}\text{C}$. The ^1H NMR

Scheme 3. Insertion of Vinyltrimethoxysilane into the Pd-CH₃ Bond of Complex t-4(Me)



signals of the bound olefinic protons appear upfield ($\delta = 5.24$, 4.99, and 4.11 ppm) of those for free VTMoS, consistent with formation of a η^2 -olefin complex rather than an O-bound complex.

Migratory insertion occurs at -40 $^{\circ}\text{C}$ yielding exclusively the 1,2-insertion product t-5(Me), which is a five-membered chelate complex involving chelation of one $-\text{OMe}$ group. Complex t-5(Me) exhibits fluxional behavior due to C–Si bond rotation and interchange of the coordinated $-\text{OMe}$ group ($\delta = 2.95$ ppm) with the two free $-\text{OMe}$ groups ($\delta = 3.54$ and 3.48 ppm). At -60 $^{\circ}\text{C}$, the rotational barrier for this process was measured via line broadening techniques ($\Delta G^\ddagger = 11.5$ kcal/mol, -60 $^{\circ}\text{C}$). In addition to the $-\text{OMe}$ resonances noted above, characteristic resonances of insertion product t-5(Me) include signals at δ 1.37 ppm and -0.82 ppm for the diastereotopic methylene protons of $\text{Pd}-\text{CH}_2$, δ 1.97 ppm for the Si–CH methine proton and δ 0.37 ppm for the methyl group at C- β of the chelate.²⁶ The first-order insertion reaction was followed by ^1H NMR spectroscopy at temperatures between -37 and -25 $^{\circ}\text{C}$. From these data, values of the activation enthalpy ($\Delta H^\ddagger = 17.4 \pm 2.2$ kcal/mol) and activation entropy ($\Delta S^\ddagger = -4.1 \pm 9.1$ eu) were obtained (Figure 3). The modest negative value of the activation entropy is consistent with an intramolecular migratory insertion reaction. At -33 $^{\circ}\text{C}$, the calculated free energy barrier ($\Delta G^\ddagger = 18.4$ kcal/mol) is only slightly higher than that of ethylene migratory insertion in the corresponding ethylene complex t-1c ($\Delta G^\ddagger = 17.8$ kcal/mol, -33 $^{\circ}\text{C}$).²⁵ Since the barrier of subsequent ethylene insertions does not differ significantly from the barrier of the first insertion of ethylene into the Pd–CH₃ bond,²⁵ we believe it is not unreasonable to use the insertion of VTMoS into a Pd–CH₃ bond as a model for insertion of VTMoS into the growing polymer chain.

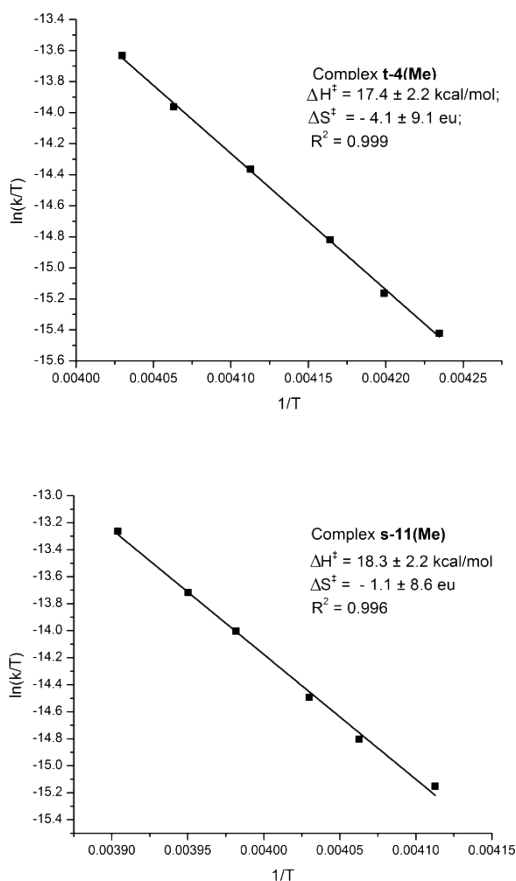
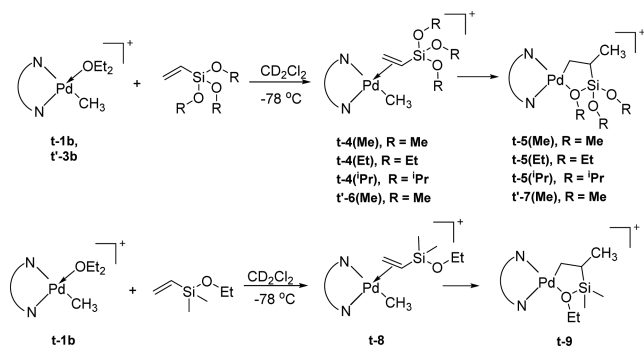


Figure 3. Eyring plots for migratory insertion of VTMoS in **t-4(Me)** and **s-11(Me)**.

In addition to VTMoS, several other vinylsilane monomers were also investigated (Scheme 4). The η^2 -olefin complexes **t-**

Scheme 4. Insertion of Vinylsilanes into the Pd–CH₃ Bonds of Traditional Vinylsilane Complexes



4(Et), **t-4(Pr)**, **t-6(Me)**, and **t-8** were generated *in situ* by treatment of the olefins with ether adducts **t-1b** and **t-3b** at -78 °C. Insertion barriers for these η^2 -olefin complexes are summarized in Table 2. VTEoS and vinyltrisopropoxysilane (VTPOs) adducts, **t-4(Et)**, **t-4(Pr)**, display similar upfield shifts of the methylenic olefinic protons. The migratory insertions of these two complexes proceed in a similar manner as that of VTMoS complex **t-4(Me)**, resulting in the formation of five-membered chelate complexes. The insertion barrier for VTEoS complex **t-4(Et)** ($\Delta G^\ddagger = 18.5$ kcal/mol at -30 °C) is similar to that for the VTMoS complex **t-4(Me)** ($\Delta G^\ddagger = 18.4$

Table 2. Migratory Insertion Barriers for Different Vinylalkoxysilane and Ethylene Complexes

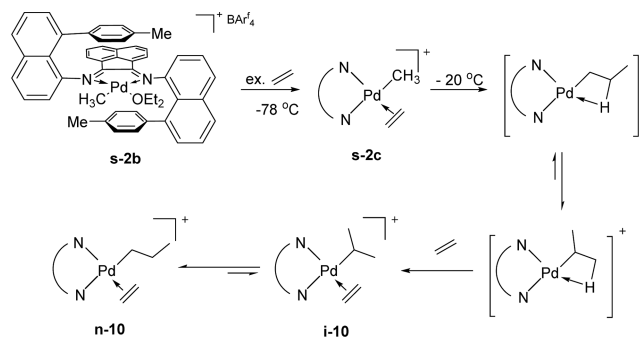
entry	olefin	olefin adduct	$T/^\circ\text{C}$	$k/\times 10^4 \text{ s}^{-1}$	ΔG^\ddagger (kcal/mol)
1	VTMoS	t-4(Me)	-30	1.4	18.4
2	VTEoS	t-4(Et)	-30	1.3	18.5
3	VTPOs	t-4(Pr)	-25	2.2	18.6
4	VDMEoS	t-8	-30	2.6	18.1
5	VTMoS	t-6(Me)	-30	0.8	18.7
6	C ₂ H ₄	t-1c	-33	3.1	17.8 ^a
7	C ₂ H ₄	s-2c	-20	1.7	19.1
8	VTMoS	s-11(Me)	-20	2.8	18.9
9	VTEoS	s-11(Et)	-20	1.4	19.2

^aAn enthalpy barrier for this case has previously been reported by Tempel et al.²⁵

kcal/mol at -30 °C). The insertion barrier for VTPOs complex **t-4(Pr)** was found to be 18.6 kcal/mol at -25 °C, ca. 0.2 kcal/mol higher than that for VTMoS complex **t-4(Me)**. The insertion barrier for vinyltrimethylethoxysilane (VDMEoS) complex **t-8** was determined to be 18.1 kcal/mol at -30 °C, ca. 0.4 kcal/mol lower than that of VTEoS complex **t-4(Et)**. The migratory insertion barrier for VTMoS complex **t-6(Me)**, which bears a less bulky ligand, was determined to be 18.7 kcal/mol, which is only ca. 0.3 kcal/mol higher than that for **t-4(Me)**. Examining entries 1–5 shows there is a negligible effect of –OR or ortho aryl substituents on barriers to migratory insertion of vinylalkoxysilanes.

In comparison to catalyst **t-1a**, the activity of sandwich catalyst **s-2a** is much lower as discussed above. The migratory insertion barriers for sandwich ethylene and vinylalkoxysilane complexes were thus investigated. Sandwich ethylene complex **s-2c** was generated *in situ* by addition of 20 equiv of ethylene to ether adduct **s-2b** (Scheme 5). At -40 °C, two broad signals at

Scheme 5. Insertion of Ethylene into the Pd–CH₃ Bond of Sandwich Complex **s-2c**

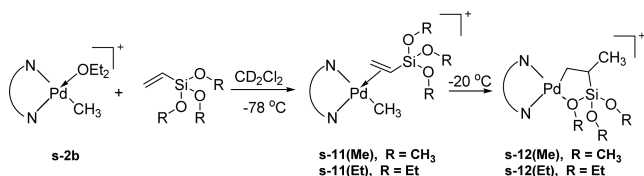


δ 4.07 and 3.95 ppm were observed for bound ethylene together with a Pd–CH₃ resonance at δ 0.25 ppm. The insertion of ethylene into the Pd–CH₃ bond is first-order, and the rate was determined by monitoring the decrease of the integral for the Pd–CH₃ signal ($\Delta G^\ddagger = 19.1$ kcal/mol at -20 °C). The ethylene complex **i-10** was obtained as the insertion product. Characteristic resonances of complex **i-10** were observed at δ 1.75 ppm (broad multiplet, PdCH(CH₃)₂), 0.73 ppm (d, $^3J_{\text{HH}} = 6.6$ Hz, PdCH(CH₃)₂), and 0.31 ppm (d, $^3J_{\text{HH}} = 6.0$ Hz, PdCH(CH₃)₂) similar to those reported for the analogous isopropyl-substituted system.²⁵ The isopropyl ethylene complex **i-10** presumably forms by trapping a β -agostic isopropyl complex, which forms via rapid isomerization of an

initially formed β -agostic *n*-propyl complex. The isopropyl ethylene complex **i-10** gradually rearranges to *n*-propyl ethylene complex **n-10** (Scheme 5). This same isomerization/trapping behavior has been found for the traditional diimine complex.²⁵

Addition of 1 equiv of VTMoS to a CD₂Cl₂ solution of **s-2b** at -78 °C leads to clean formation of two isomers of η^2 -VTMoS complex **s-11(Me)** in a 3:2 ratio (Scheme 6). Key ¹H

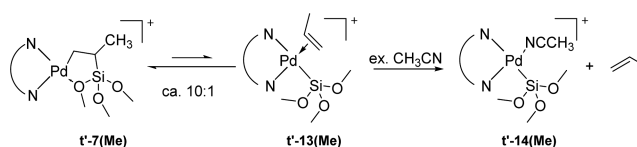
Scheme 6. Insertion of Vinylsilanes into the Pd–CH₃ Bonds of **s-11**



NMR resonances for the major isomer include signals at $\delta = 4.52, 4.44,$ and 3.56 ppm for the bound olefinic protons and $\delta = 0.44$ ppm for the Pd–CH₃ methyl group. Resonances attributable to the minor isomer were observed at $\delta = 4.82, 4.70, 3.27$ ppm for bound olefinic protons and $\delta = 0.52$ ppm for the Pd–CH₃ methyl group. Upon warming to -40 °C, a 1:1 equilibrium ratio of isomers is generated. Similar to complex **t-4(Me)**, migratory insertion of VTMoS complex **s-11(Me)** occurs in a 1,2 fashion to form a five-membered chelate complex, but the case here is complicated by the fact the α -diimine ligand possesses C₂ symmetry and two isomeric five-membered chelates can be formed. Only one chelate isomer was fully distinguishable by NMR, due to overlapping and complex resonances. Key ¹H NMR resonances of the major chelate isomer include signals at $\delta 1.32$ and -0.95 ppm for the diastereotopic methylene protons of Pd–CH₂, $\delta 1.61$ ppm for the Si–CH methine proton and $\delta 0.38$ ppm for the methyl group on the chelate. The migratory insertion reaction of the VTMoS complex **s-11(Me)** was observed at -20 °C by monitoring the disappearance of Pd–CH₃ methyl resonances. First-order kinetics were observed with $k_{\text{ins}} = 2.8 \times 10^{-4} \text{ s}^{-1}$ ($\Delta G^\ddagger = 18.9$ kcal/mol). Figure 3 shows an Eyring plot for this insertion reaction over the range -30 to -17 °C in CD₂Cl₂. The activation enthalpy (ΔH^\ddagger) is 18.3 ± 2.2 kcal/mol, while the activation entropy (ΔS^\ddagger) is -1.1 ± 8.6 eu. The near-zero value of ΔS^\ddagger is consistent with an intramolecular migratory insertion. The insertion barrier ($\Delta G^\ddagger = 18.9$ kcal/mol, -20 °C) is roughly the same as that for ethylene insertion ($\Delta G^\ddagger = 19.1$ kcal/mol, -20 °C) in complex **s-2c** and ca. 0.5 kcal/mol higher than that of VTMoS insertion in the isopropyl complex **t-4(Me)** ($\Delta G^\ddagger = 18.4$ kcal/mol, -30 °C). The corresponding VTEoS complex **s-11(Et)** displays similar spectral features to the VTMoS analogue **s-11(Me)**, including the occurrence of two isomers. At -20 °C, VTEoS inserts into the Pd–CH₃ bond with $k_{\text{ins}} = 1.4 \times 10^{-4} \text{ s}^{-1}$ ($\Delta G^\ddagger = 19.2$ kcal/mol) to afford chelate complexes. The insertion barrier is ca. 0.3 kcal/mol higher than that for VTMoS complex **s-11(Me)** ($\Delta G^\ddagger = 18.9$ kcal/mol, -20 °C) and almost the same as that for sandwich ethylene complex **s-2c** ($\Delta G^\ddagger = 19.1$ kcal/mol, -20 °C).

Evidence for β -Silyl Elimination. At higher temperatures, β -silyl elimination in methyl-substituted traditional complex **t'-7(Me)** was observed forming a silyl propylene complex, **t'-13(Me)** (Scheme 7).²⁷ Characteristic resonances of bound propylene in complex **t'-13(Me)** include $\delta 5.44, 4.51,$ and 4.21 ppm for the olefinic protons and $\delta 1.76$ ppm for the methyl

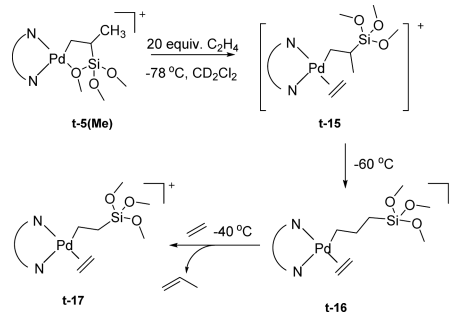
Scheme 7. β -Silyl Elimination Observed for Chelate Complex **t'-7(Me)**



protons. The ratio of complex **t'-7(Me)** and β -silyl elimination product **t'-13(Me)** is ca. 10:1 at -25 °C. The addition of excess acetonitrile to an NMR sample of **t'-7(Me)**/**t'-13(Me)** results in the quantitative formation of free propylene (¹H NMR: 5.80, 5.00, 4.89, and 1.67 ppm) and silyl acetonitrile complex **t'-14(Me)** (Scheme 7). In contrast to the methyl-substituted complex **t'-7(Me)**, the more bulky isopropyl-substituted complex **t-5(Me)** forms a much smaller fraction (<5%) of β -silyl elimination product. Notably, no β -silyl elimination product could be detected in the case of the sandwich complex **s-12(Me)** even at 0 °C.

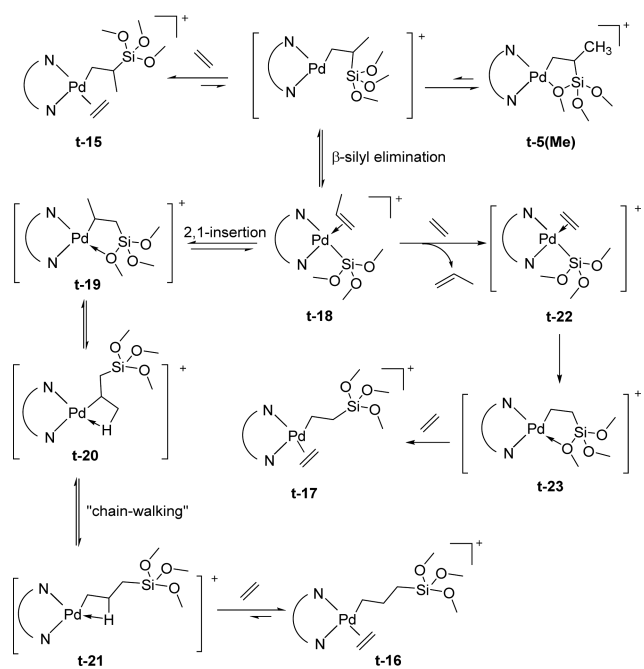
Chelate Opening with Ethylene and Chain Transfer. Addition of 20 equiv of ethylene to the CD₂Cl₂ solution of isopropyl-substituted complex **t-5(Me)** at -78 °C results in rapid formation of a new complex proposed to be **t-15** (Scheme 8). Warming from -78 to -60 °C, complex **t-15** rapidly

Scheme 8. Chelate Opening of Complex **t-5(Me) with Ethylene**



isomerizes to the linear silylpropyl ethylene complex **t-16**. Characteristic resonances of complex **t-16** were observed at $\delta 1.52$ ppm (*t*, ³J_{HHH} = 8.4 Hz, PdCH₂CH₂CH₂Si(OMe)₃), 1.05 ppm (broad multiplet, PdCH₂CH₂CH₂Si(OMe)₃), and 0.17 ppm (*t*, ³J_{HHH} = 8.4 Hz, PdCH₂CH₂CH₂Si(OMe)₃). Upon warming to -40 °C, further rearrangement of complex **t-16** to silylethyl ethylene complex **t-17** was observed, along with formation of ca. 1 equiv of free propylene (Scheme 8). The formation of **t-17** was clearly indicated by the presence of two triplets at $\delta 1.74$ (PdCH₂) and $\delta 0.42$ (SiCH₂) ppm assigned to the two sets of methylene protons.

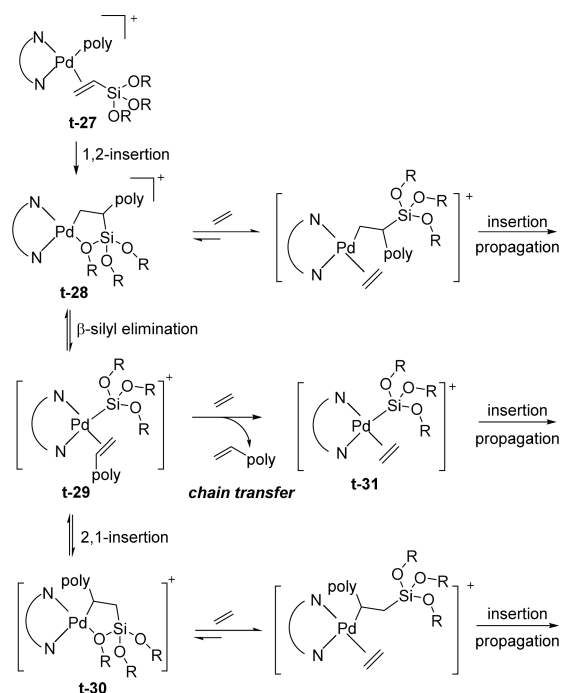
The mechanism proposed for formation of **t-16** and **t-17** is shown in Scheme 9. Loss of ethylene from complex **t-15** (or opening of chelate complex **t-5(Me)**) followed by β -silyl elimination results in the formation of trimethoxysilyl η^2 -propylene intermediate **t-18**. Intermediate **t-18** undergoes a 2,1-migratory insertion to yield **t-19**.²⁷ Subsequent “chain walking” via intermediate **t-20** yields the observed silylpropyl ethylene complex **t-16**. If all steps are rapid and reversible, low concentrations of intermediate **t-18** can be intercepted by ethylene to form **t-22** and (observed) propylene. Insertion of ethylene to the Pd-silyl bond of **t-22** leads to a five-membered chelate intermediate **t-23**. Reaction of ethylene (present in

Scheme 9. Proposed Mechanism of Formation of Complexes **t-16** and **t-17**

excess) with intermediate **t-23** opens the chelate to generate the observed silyl ethylene complex **t-17**.

Ethylene complex **t-17** in the presence of excess ethylene at $-25\text{ }^{\circ}\text{C}$ undergoes chain growth along with formation of some 1-butene and minor amounts of higher α -olefins.²⁴ Thus, the picture that emerges for initiation and continued chain growth is shown in Scheme 10. As the alkyl chain grows longer, the rate at which chain-walking moves the silyl group to the β position (necessary for β -silyl elimination) decreases relative to the rate of ethylene insertion. Thus, elimination and formation of higher α -olefins will rapidly decrease as the alkyl chain grows.

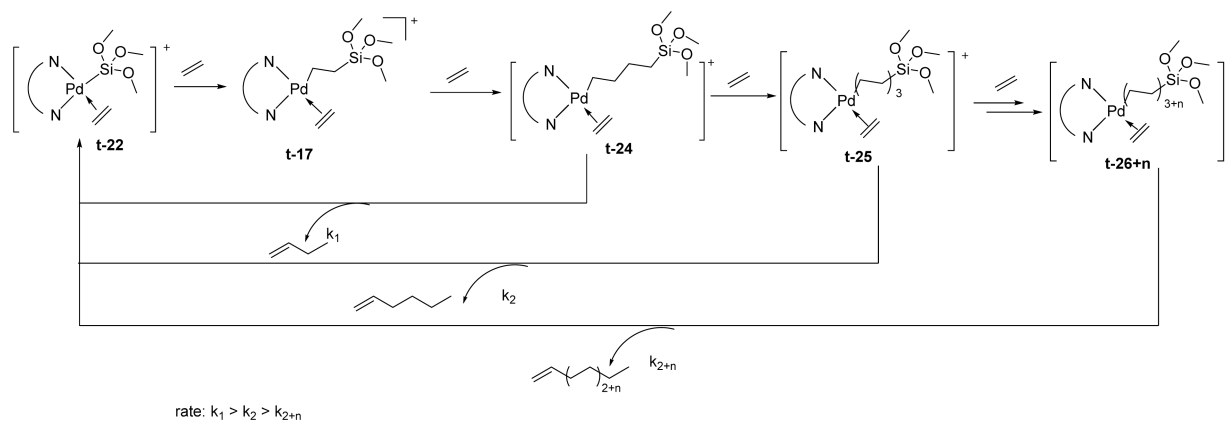
It is clear from the above results that β -silyl elimination serves as the chain transfer mechanism and results in the low molecular weight of copolymers if catalyst **t-1** is used (Scheme 11). After chain growth via a series of ethylene insertions, trapping of this species by the vinylsilane would yield a π -complex of type **t-27**. 1,2-Insertion of the vinylsilane would yield a five-membered chelate **t-28** which can undergo β -silyl elimination to generate **t-29**. Chain transfer is completed via

Scheme 11. Proposed Chain Transfer Process via a β -Silyl Elimination Mechanism

associative displacement of the unsaturated chain by ethylene to yield the silyl ethylene complex, **t-31**, which can initiate growth of a new chain as shown above. Species **t-29** could undergo 2,1 insertion to yield **t-30**, but ultimately, reversible β -silyl elimination will reform **t-29**. Chain transfer via this pathway will result in formation of copolymers with a terminal olefin end group which matches well with the end group analysis of these copolymers obtained in copolymerization experiments (Table 1). This mechanism also accounts for the incorporation of one $-\text{Si}(\text{OR})_3$ group per chain.

In the case on the sandwich system, we have established that associative displacement of bound ethylene by free ethylene from a sandwich Pd(II) alkyl ethylene complex is at least 5 orders of magnitude slower than the same displacement reaction in the traditional catalyst system.²⁰ This feature results in polyethylene formed from these catalysts having very narrow molecular weight distributions. On this basis, we would expect that the rate of chain transfer via the β -silyl mechanism would

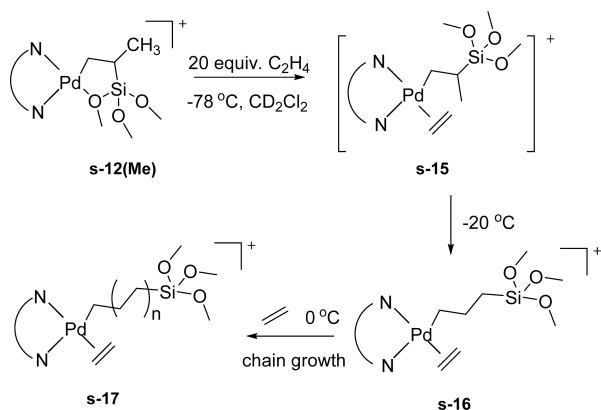
Scheme 10. Proposed Mechanism of Chain Growth in the Traditional Catalyst System



be greatly diminished in these copolymerizations. Slow chain transfer is supported by the observation that copolymers formed from sandwich catalyst **s-2a** have very narrow molecular weight distributions, copolymers can be generated with considerably higher molecular weights than with **t-1a**, and several vinyltrialkoxysilane units can be incorporated per chain.

Additional low temperature NMR experiments confirm this hypothesis. Addition of 20 equiv of ethylene to a CD_2Cl_2 solution of sandwich chelate complex **s-12(Me)** at $-78\text{ }^\circ\text{C}$ results in complete opening of the chelate to form two isomers of the ethylene complex **s-15** (Scheme 12). Again, the C_2

Scheme 12. Chelate Opening with Ethylene in Sandwich Complex **s-12(Me)**



symmetry of the ligand and the chiral center α to Si results in formation of two isomers. Upon warming to $-20\text{ }^\circ\text{C}$, the silylpropyl ethylene complex **s-16** was observed (in analogy with **t-16**) which is readily identified by ^1H NMR analysis. The characteristic resonances of complex **s-16** are seen at δ 0.93 ppm ($\text{PdCH}_2\text{CH}_2\text{CH}_2\text{Si}(\text{OMe})_3$), -0.03 ppm (broad multiplets, $\text{PdCH}_2\text{CH}_2\text{CH}_2\text{Si}(\text{OMe})_3$), and -0.62 ppm ($t, {}^3J_{\text{HH}} = 12.0$ Hz, $\text{PdCH}_2\text{CH}_2\text{CH}_2\text{Si}(\text{OMe})_3$). Complex **s-16** reacts with ethylene and alkyl chain growth ensues as evidenced by the disappearance of the signals of **s-16** and the decrease in the ethylene resonance. A key point is that *no free propylene was detected even at $0\text{ }^\circ\text{C}$* . Thus, while β -silyl elimination must occur in converting **s-15** to **s-16** via a silyl propylene complex, propylene is not displaced by ethylene but rather chain growth via ethylene insertion ensues.²⁸ These observations establish that the rate of chain transfer via the β -silyl mechanism is very greatly retarded in this sandwich catalyst system due to the very slow associative displacement of olefins from any silyl olefin complex intermediates.

Chain Propagation. Since chelate opening by ethylene is extremely rapid and no observable chelate is detected in the presence of ethylene, it is clear that alkyl ethylene complexes are the catalyst resting states. The rate of migratory insertion of ethylene controls the turnover frequency which will be zero-order in ethylene. The turnover frequencies for the two catalysts were determined by NMR spectroscopy by measuring the decreasing signal for free ethylene in solution (Table 3).²⁵ The numbers are consistent with values determined for homopolymerizations of ethylene where the alkyl ethylene complexes are the resting states. For the isopropyl-substituted system **t-17**, the average rate of ethylene insertion was measured at $-25\text{ }^\circ\text{C}$ and the corresponding activation barrier, ΔG^\ddagger , was determined to be 18.4 kcal/mol, which is, as

Table 3. Average Rates for Subsequent Ethylene Insertions

entry	olefin	initiating complex	$T/^\circ\text{C}$	$k/\times 10^4\text{ s}^{-1}$	ΔG^\ddagger (kcal/mol)
1	VTMoS	t-17	-25	3.1	18.4
2	C_2H_4	t-1c	-28	5.6	17.9 ^a
3	VTMoS	s-16	0	5.8	20.0
4	C_2H_4	s-2c	0	6.7	19.9

^aThis barrier has also been measured to be $\Delta G^\ddagger = 18.0$ kcal/mol, $-26\text{ }^\circ\text{C}$ by Tempel et al.²⁵

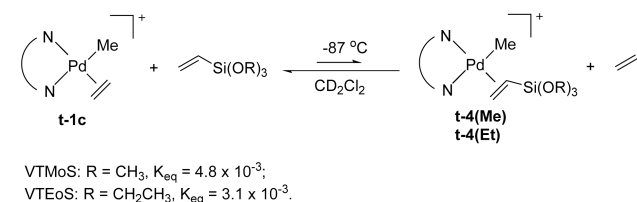
expected, nearly the same as that for ethylene homopolymerization, $\Delta G^\ddagger = 17.9$ kcal/mol at $-28\text{ }^\circ\text{C}$.²⁵

For the sandwich complex **s-16**, the rate constant for ethylene insertion was determined to be $5.8 \times 10^{-4}\text{ s}^{-1}$ at $0\text{ }^\circ\text{C}$ ($\Delta G^\ddagger = 20.0$ kcal/mol). This barrier is the same as that for ethylene homopolymerization ($\Delta G^\ddagger = 19.9$ kcal/mol, $0\text{ }^\circ\text{C}$) and ca. 1.6 kcal/mol higher than that of the isopropyl system **t-17** ($\Delta G^\ddagger = 18.4$ kcal/mol, $-25\text{ }^\circ\text{C}$).

Relative Binding Constants. In the copolymerization of ethylene and methyl acrylate using traditional α -diimine catalysts, where ligand exchange is faster than insertion, the incorporation ratio of ethylene vs MA into the copolymer is determined by their relative insertion rates, their relative binding affinities, and their relative concentrations in solution.⁸ Given that the insertion barriers of vinylalkoxysilanes are comparable to those of ethylene, the relative binding affinities of vinyltrialkoxysilanes and ethylene become a key factor in determining the incorporation ratio aside from the concentration difference in the solution of ethylene and the vinylalkoxysilane.

For the isopropyl catalyst system, **t-1**, equilibrium constants for the reaction depicted in Scheme 13 were measured by low-

Scheme 13. Relative Binding Affinities of Ethylene and Vinylalkoxysilanes



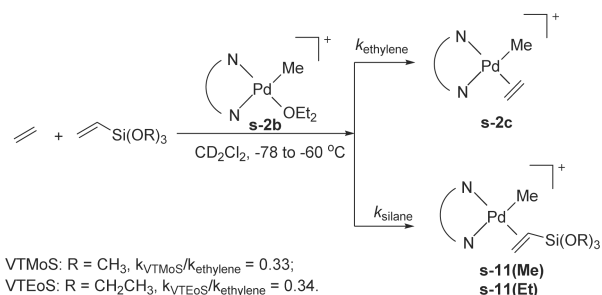
temperature ^1H NMR spectroscopy. Results show that ethylene binds more strongly than vinyltrialkoxysilanes, presumably due to steric factors. For VTMoS, the equilibrium constant (K_{eq}) is 4.8×10^{-3} at $-87\text{ }^\circ\text{C}$ ($\Delta G = 2.0$ kcal/mol), while, for vinyltriethoxysilane (VTEoS), the equilibrium constant is slightly smaller, $K_{\text{eq}} = 3.1 \times 10^{-3}$, $\Delta G = 2.1$ kcal/mol. In comparison to the binding affinity of methyl acrylate where an analogous $K_{\text{eq}} = 1.0 \times 10^{-6}$ ($-95\text{ }^\circ\text{C}$),⁸ the vinyltrialkoxysilanes bind ca. 1000 times more strongly. Extrapolating the above data to the temperature of the copolymerization reactions ($22\text{ }^\circ\text{C}$) and assuming $\Delta S = 0$, the equilibrium constants calculated are 0.033 and 0.028, respectively, which favor ethylene but not to such a high degree to exclude significant polar monomer incorporation.

By extrapolation of these data to the temperature of the copolymerization reaction ($22\text{ }^\circ\text{C}$), we find good agreement with the incorporation ratio observed in copolymerization of ethylene with VTEoS. Eyring analyses have not been carried out for the ethylene and VTEoS insertions, but assuming a

similar ΔS^\ddagger to that for VTMoS complex **t-4(Me)** (-4.1 ± 9.1 eu) and using the measured ΔG^\ddagger at -30 °C (18.5 kcal/mol) for VTEoS complex **t-4(Et)** and the measured barrier for ethylene insertion at -33 °C (17.8 kcal/mol), barriers for insertion of VTEoS and ethylene at 22 °C can be estimated as ca. 18.7 and 18.0 kcal/mol, respectively. The estimated difference between these two insertion barriers at 22 °C of ca. 0.7 kcal/mol corresponds to a rate ratio $k_{\text{VTEoS}}/k_{\text{ethylene}}$ of ca. 0.3. Multiplying this insertion rate ratio by the relative binding affinities and taking into account the olefin concentrations in entry 1, Table 1 (i.e., $[\text{VTEoS}] = 0.52$ M, $[\text{Ethylene}] = 1.39$ M),²⁹ a VTEoS incorporation ratio of ca. 0.31 mol % is predicted, which agrees reasonably well with that of 0.26 mol % observed.

As for the sandwich catalyst system, attempted measurement of the equilibrium of **s-2c** and **s-11(Me)** (or **s-11(Et)**) at low temperatures was unsuccessful due to the extremely slow exchange rates and the fact that migratory insertions of these complexes are faster than ligand exchanges. We can, however, measure the relative kinetic trapping rates of ether complex **s-2b** by vinyltrialkoxysilanes versus ethylene to yield complexes **s-2c** and **s-11(Me)** or **s-11(Et)** as shown in Scheme 14. For

Scheme 14. Relative Trapping Rates of Ethylene and Vinyltrialkoxysilanes



vinyltrimethoxysilane (VTMoS), the relative trapping rate $k_{\text{VTMoS}}/k_{\text{ethylene}}$ is ca. 0.33 at -60 °C, while that of VTEoS is essentially the same, ca. 0.34 at -60 °C. These relative trapping rates are ca. 10 times greater than relative binding affinities for the traditional complex at 22 °C, which might account for the higher incorporation ratio (ca. 2 times) of VTEoS in the copolymer produced by the “sandwich” complex **s-2a** relative to complex **t-1a**, despite the fact that **s-2a** contains the more crowded binding site.^{30,31} We cannot estimate what the incorporation level of vinyltrialkoxysilanes should be as we do not know what the trapping ratios of the bulkier β -agostic alkyl intermediates³² will be relative to the ether complexes **s-2b**. Furthermore, some displacement of the more weakly binding vinylsilane may be competitive with insertion under the polymerization conditions. But, nonetheless, slow olefin exchange coupled with favorable kinetic trapping ratios provides a potential rationale for the observation that greater levels of the vinylsilanes can be incorporated into copolymers produced using the bulkier sandwich catalysts.

CONCLUSIONS

The α -diimine Pd(II) catalysts **t-1a** and **s-2a** exhibit functional group tolerance and allow for the copolymerization of ethylene with vinyltrialkoxysilanes to yield highly branched copolymers at rates similar to those for the homopolymerization of ethylene. This behavior is in contrast to the copolymerization of ethylene with methyl acrylate using these catalysts where

rates are significantly reduced relative to the ethylene homopolymerizations. Studies reported here have exposed numerous mechanistic features of the chain growth and termination processes which together provide a rationale for the behavior of these copolymerizations reactions. Key points are summarized below:

- (1) The traditional catalyst **t-1a** copolymerizes ethylene with VTEoS to give highly branched functionalized polyethylene. In comparison to copolymerization of ethylene with methyl acrylate, the rate of copolymerization of ethylene with VTEoS is much higher and comparable to that of ethylene homopolymerization, but at the same time, molecular weights of the copolymers are much lower than those of the homopolymer.
- (2) The cationic (α -diimine)PdMe(OEt₂)⁺ complexes react rapidly with vinyltrimethoxysilane (VTMoS) to form η^2 -olefin complexes at -78 °C. Migratory insertion of VTMoS into the Pd–CH₃ bond occurs regioselectively in a 1,2 fashion to yield five-membered chelates. Insertion barriers of VTMoS were determined and found to be only slightly higher than those for ethylene insertions. Thus, slow insertion rates of the comonomer are not a factor in retarding the levels of comonomer incorporation.
- (3) The five-membered chelates formed from VTMoS insertion are very rapidly opened at -78 °C by ethylene to form Pd(II) ethylene alkyl complexes. Equilibrium between the chelates and the opened alkyl ethylene complexes strongly favors the opened ethylene alkyl species. Thus, copolymerization rates are not retarded by chelate formation. This behavior is in contrast to MA where the chelate generated from MA insertion is favored over the open alkyl ethylene complex.
- (4) For traditional catalyst **t-1b**, associative exchange of olefins is rapid relative to insertion; thus, the fraction of vinylsilane incorporation is determined by the relative binding affinities of the two monomers coupled with their relative insertion rates (Curtin–Hammett kinetics). Under polymerization conditions, the ratio of insertion rates, $k_{\text{VTEoS}}/k_{\text{ethylene}}$, was estimated as ca. 0.3 and the relative binding affinity of the vinyltrialkoxysilanes and ethylene was ca. 0.03. By taking into account monomer concentrations, the estimated VTEoS incorporation for entry 1, Table 1 is 0.31 mol % in reasonable agreement with the observed value of 0.26 mol %. This level of incorporation is sufficient to effect cross-linking. In the case of the sandwich complex, the exchange rates of olefins are quite slow; thus, silane incorporation levels are determined, at least in part, by relative rates of trapping of the cationic β -agostic alkyl complexes. The relative rates ($k_{\text{silane}}/k_{\text{ethylene}}$) of trapping the methyl diethyl ether complex **s-2b** are ca. 0.3, which favor ethylene, and have a smaller difference between silanes and ethylene than the relative binding affinities.³³ This feature results, surprisingly, in a higher level of incorporation of the vinyltrialkoxysilanes into the copolymers relative to the traditional catalysts, even though the sandwich catalysts possess more hindered coordination sites.
- (5) For the traditional catalyst **t-1a**, each copolymer chain produced contains one vinyltrialkoxysilane unit and the copolymer molecular weights decrease as the concentration of the vinyltrialkoxysilane increases. The M_w/M_n

values of these polymers are ca. 2 showing the M_n values are chain-transfer limited. Low temperature NMR studies established that the chelate intermediates undergo facile β -silyl elimination with associative displacement of the formed olefin by ethylene. Thus, insertion of vinyltrialkoxysilane into a growing chain results in chain transfer and initiation of a new chain via silane insertion; each chain produced bears a $-\text{Si}(\text{OR})_3$ end group. For the sandwich catalyst β -silyl elimination could occur, but the formed olefin is not displaced. Thus, the vinylsilane monomers do not induce rapid chain transfer, high molecular weight polymers can be produced with narrow molecular weight distributions, and many vinyltrialkoxysilane monomers can be incorporated into a single chain.

Due to the high cost of palladium and the relative low activities of these catalysts, they hold little industrial interest. We are currently extending mechanistic and preparative studies to nickel analogs that show much higher activities.

■ ASSOCIATED CONTENT

Supporting Information

The Supporting Information is available free of charge on the ACS Publications website at DOI: 10.1021/jacs.6b10462.

Detailed experimental procedures, characterization data for complexes **t-1b**, **s-2b,c**, **t-4,5,8,9,16,17**, **t'-6,7**, **s-11,12,16**; ^1H NMR spectra of copolymer; and kinetic plots (PDF)

■ AUTHOR INFORMATION

Corresponding Authors

*mbrookhart@unc.edu

*olafs@uh.edu

ORCID

Zhou Chen: 0000-0003-4345-7070

Present Address

§Canon Nanotechnologies, Inc., Austin, TX 78758.

Notes

The authors declare no competing financial interest.

■ ACKNOWLEDGMENTS

This research was supported by the National Science Foundation (CHE-1010170 to M.B.) and the Welch Foundation (Chair E-0044 to O.D. and Grant E-1893 to M.B.).

■ REFERENCES

- (1) (a) Ittel, S. D.; Johnson, L. K.; Brookhart, M. *Chem. Rev.* **2000**, *100*, 1169–1203. (b) Boffa, L. S.; Novak, B. M. *Chem. Rev.* **2000**, *100*, 1479–1493. (c) Chung, T. C. *Prog. Polym. Sci.* **2002**, *27*, 39–85. (d) Berkefeld, A.; Mecking, S. *Angew. Chem., Int. Ed.* **2008**, *47*, 2538–2542. (e) Nakamura, A.; Ito, S.; Nozaki, K. *Chem. Rev.* **2009**, *109*, 5215–5244. (f) Boardman, B. M.; Bazan, G. C. *Acc. Chem. Res.* **2009**, *42*, 1597–1606. (g) Takeuchi, D. *Dalton Trans.* **2010**, *39*, 311–328.
- (2) (a) Chung, T. C. *Macromolecules* **1988**, *21*, 865–869. (b) Kesti, M. R.; Coates, G. W.; Waymouth, R. M. *J. Am. Chem. Soc.* **1992**, *114*, 9679–9680. (c) Terao, H.; Ishii, S.; Mitani, M.; Tanaka, H.; Fujita, T. *J. Am. Chem. Soc.* **2008**, *130*, 17636–17637. (d) Yang, X.-H.; Liu, C.-R.; Wang, C.; Sun, X.-L.; Guo, Y.-H.; Wang, X.-K.; Wang, Z.; Xie, Z.; Tang, Y. *Angew. Chem., Int. Ed.* **2009**, *48*, 8099–8102. (e) Hong, M.; Wang, Y.-X.; Mu, H.-L.; Li, Y.-S. *Organometallics* **2011**, *30*, 4678–4686. (f) Chen, Z.; Li, J.-F.; Tao, W.-J.; Sun, X.-L.; Yang, X.-H.; Tang,

Y. *Macromolecules* **2013**, *46*, 2870–2875. (g) Wang, X.; Wang, Y.; Shi, X.; Liu, J.; Chen, C.; Li, Y. *Macromolecules* **2014**, *47*, 552–559.

- (3) (a) Younkin, T. R.; Connor, E. F.; Henderson, J. I.; Friedrich, S. K.; Grubbs, R. H.; Bansleben, D. A. *Science* **2000**, *287*, 460–462. (b) Diamanti, S. J.; Ghosh, P.; Shimizu, F.; Bazan, G. C. *Macromolecules* **2003**, *36*, 9731–9735. (c) Zuideveld, M. A.; Wehrmann, P.; Röhr, C.; Mecking, S. *Angew. Chem., Int. Ed.* **2004**, *43*, 869–873.

- (4) (a) Johnson, L. K.; Mecking, S.; Brookhart, M. *J. Am. Chem. Soc.* **1996**, *118*, 267–268. (b) Drent, E.; van Dijk, R.; van Ginkel, R.; van Oort, B.; Pugh, R. I. *Chem. Commun.* **2002**, 744–745. (c) Guironnet, D.; Roesle, P.; Rünzi, T.; Göttker-Schnetmann, I.; Mecking, S. *J. Am. Chem. Soc.* **2009**, *131*, 422–423.

- (5) Ito, S.; Munakata, K.; Nakamura, A.; Nozaki, K. *J. Am. Chem. Soc.* **2009**, *131*, 14606–14607.

- (6) Kochi, T.; Noda, S.; Yoshimura, K.; Nozaki, K. *J. Am. Chem. Soc.* **2007**, *129*, 8948–8949.

- (7) (a) Luo, S.; Jordan, R. F. *J. Am. Chem. Soc.* **2006**, *128*, 12072–12073. (b) Luo, S.; Vela, J.; Lief, G. R.; Jordan, R. F. *J. Am. Chem. Soc.* **2007**, *129*, 8946–8947. (c) Weng, W.; Shen, Z.; Jordan, R. F. *J. Am. Chem. Soc.* **2007**, *129*, 15450–15451. (d) Rünzi, T.; Fröhlich, D.; Mecking, S. *J. Am. Chem. Soc.* **2010**, *132*, 17690–17691. (e) Sui, X.; Dai, S.; Chen, C. *ACS Catal.* **2015**, *5*, 5932–5937. (f) Schuster, N.; Rünzi, T.; Mecking, S. *Macromolecules* **2016**, *49*, 1172–1179.

- (8) Mecking, S.; Johnson, L. K.; Wang, L.; Brookhart, M. *J. Am. Chem. Soc.* **1998**, *120*, 888–899.

- (9) Nakamura, A.; Anselment, T. M. J.; Claverie, J.; Goodall, B.; Jordan, R. F.; Mecking, S.; Rieger, B.; Sen, A.; van Leeuwen, P. W. N. M.; Nozaki, K. *Acc. Chem. Res.* **2013**, *46*, 1438–1449.

- (10) (a) Zhou, X.; Jordan, R. F. *Organometallics* **2011**, *30*, 4632–4642. (b) Gott, A. L.; Piers, W. E.; Dutton, J. L.; McDonald, R.; Parvez, M. *Organometallics* **2011**, *30*, 4236–4249. (c) Wucher, P.; Roesle, P.; Falivene, L.; Cavallo, L.; Caporaso, L.; Göttker-Schnetmann, I.; Mecking, S. *Organometallics* **2012**, *31*, 8505–8515. (d) Contrella, N. D.; Sampson, J. R.; Jordan, R. F. *Organometallics* **2014**, *33*, 3546–3555. (e) Zhang, Y.; Cao, Y.; Leng, X.; Chen, C.; Huang, Z. *Organometallics* **2014**, *33*, 3738–3745. (f) Nakano, R.; Nozaki, K. *J. Am. Chem. Soc.* **2015**, *137*, 10934–10937. (g) Jian, Z.; Falivene, L.; Wucher, P.; Roesle, P.; Caporaso, L.; Cavallo, L.; Göttker-Schnetmann, I.; Mecking, S. *Chem. - Eur. J.* **2015**, *21*, 2062–2075.

- (11) (a) Carrow, B. P.; Nozaki, K. *J. Am. Chem. Soc.* **2012**, *134*, 8802–8805. (b) Long, B. K.; Eagan, J. M.; Mulzer, M.; Coates, G. W. *Angew. Chem., Int. Ed.* **2016**, *55*, 7106–7110. (c) Tao, W.-j.; Nakano, R.; Ito, S.; Nozaki, K. *Angew. Chem., Int. Ed.* **2016**, *55*, 2835–2839. (d) A recent report showed that a cationic Pd(II) catalyst based on a bidentate phosphine/phosphine oxide catalyst shows only a small drop (ca. 3 times) in the rate of ethylene/methyl acrylate copolymerization relative to ethylene homopolymerization: Mitsushige, Y.; Carrow, B. P.; Ito, S.; Nozaki, K. *Chem. Sci.* **2016**, *7*, 737–744.

- (12) Williams, B. S.; Leatherman, M. D.; White, P. S.; Brookhart, M. *J. Am. Chem. Soc.* **2005**, *127*, 5132–5146.

- (13) (a) Tsunaga, M.; Matsunami, S.; Sato, M.; Nakata, K. *Plast., Rubber Compos.* **1998**, *27*, 460–464. (b) Rizzo, P.; Baione, F.; Guerra, G.; Martinotto, L.; Albizzati, E. *Macromolecules* **2001**, *34*, 5175–5179. (c) Khonakdar, H. A.; Morshedjan, J.; Wagenknecht, U.; Jafari, S. H. *Polymer* **2003**, *44*, 4301–4309.

- (14) (a) Scott, H. G. U.S. 3646155, 1972. (b) Narkis, M.; Tzur, A.; Vaxman, A.; Fritz, H. G. *Polym. Eng. Sci.* **1985**, *25*, 857–862.

- (15) Kawakami, T.; Ito, S.; Nozaki, K. *Dalton Trans.* **2015**, *44*, 20745–20752.

- (16) (a) Amin, S. B.; Marks, T. J. *J. Am. Chem. Soc.* **2006**, *128*, 4506–4507. (b) Liu, J.; Nomura, K. *Macromolecules* **2008**, *41*, 1070–1072. (c) Nomura, K.; Kakinuki, K.; Fujiki, M.; Itagaki, K. *Macromolecules* **2008**, *41*, 8974–8976. (d) Zimmer, S.; Schöbel, A.; Halbach, T.; Stohrer, J.; Rieger, B. *Macromol. Rapid Commun.* **2013**, *34*, 221–226.

- (17) Johnson, L. K.; McLain, S. J.; Sweetman, K. J.; Wang, Y.; Bennett, A. M. A.; Wang, L.; McCord, E. F.; Lonkin, A.; Ittel, S. D.; Radzewich, C. E.; Schifano, R. S. WO 2003044066, 2003.

(18) (a) Camacho, D. H.; Salo, E. V.; Ziller, J. W.; Guan, Z. *Angew. Chem., Int. Ed.* **2004**, *43*, 1821–1825. (b) Cherian, A. E.; Rose, J. M.; Lobkovsky, E. B.; Coates, G. W. *J. Am. Chem. Soc.* **2005**, *127*, 13770–13771. (c) Meinhard, D.; Wegner, M.; Kipiani, G.; Hearley, A.; Reuter, P.; Fischer, S.; Marti, O.; Rieger, B. *J. Am. Chem. Soc.* **2007**, *129*, 9182–9191. (d) Liu, J.; Chen, D.; Wu, H.; Xiao, Z.; Gao, H.; Zhu, F.; Wu, Q. *Macromolecules* **2014**, *47*, 3325–3331. (e) Zou, W.; Chen, C. *Organometallics* **2016**, *35*, 1794–1801.

(19) Johnson, L. K.; Killian, C. M.; Brookhart, M. *J. Am. Chem. Soc.* **1995**, *117*, 6414–6415.

(20) Allen, K. E.; Campos, J.; Daugulis, O.; Brookhart, M. *ACS Catal.* **2015**, *5*, 456–464.

(21) NMR analysis of these highly branched copolymers prepared using the “traditional” catalyst **t-1a** and “sandwich” catalyst **s-2a** establish a $-\text{CH}_2\text{Si}(\text{OEt})_3$ (δ 0.56–0.65 ppm) end group and the structure is in accordance with the copolymer produced by the palladium catalyst in ref 17.

(22) Similar data of Pd-catalyzed copolymerization of ethylene (100 psig) and VTEoS [0.52 M] at 30 °C are reported in ref 17. The molecular weight of the copolymer produced is ca. 8.0×10^3 g/mol, which is comparable with the values reported in Table 1 of this report.

(23) The fact that these chains possess only a single $-\text{Si}(\text{OEt})_3$ group means that cross-linking will result in dimerization or 3- or 4-armed stars, not a traditional cross-linked network.

(24) As shown in Scheme 10, upon insertion of vinyl silane and prior to polymer chain growth a distribution of low M_n α -olefins are formed. Since these low molecular weight olefins are not isolated, their formation may account for the small decrease in TOFs (based on mass of isolated polymer) relative to the homopolymerizations. These linear α -olefins (specifically, 1-hexene and 1-octene) were observed in the copolymerization described in entry 3, Table 1.

(25) Tempel, D. J.; Johnson, L. K.; Huff, R. L.; White, P. S.; Brookhart, M. *J. Am. Chem. Soc.* **2000**, *122*, 6686–6700.

(26) Small amounts (less than 10%) of an unidentified complex was also observed during the insertion.

(27) LaPointe, A. M.; Rix, F. C.; Brookhart, M. *J. Am. Chem. Soc.* **1997**, *119*, 906–917.

(28) In copolymerization reactions using catalyst **s-2a**, nearly all silyl groups in copolymer have a $-\text{CH}_2\text{Si}(\text{OEt})_3$ structure. One mechanism for this structure was proposed in analogy with the mechanism shown in Scheme 11. After 1,2-insertion of VTEoS, the $\text{PdCH}_2\text{CH}(\text{poly})\text{Si}(\text{OEt})_3$ sandwich complex formed must undergo β -silyl elimination to generate $\text{Pd}(\text{CH}_2=\text{CHpoly})(\text{Si}(\text{OEt})_3)$, followed by 2,1-insertion to form $\text{PdCH}(\text{poly})\text{CH}_2\text{Si}(\text{OEt})_3$ (in analogy with complex **t-30**, Scheme 11), which can undergo chain-walking or propagation.

(29) It is assumed that the solubility of ethylene in VTEoS is similar to that in methylene chloride. The solubility of ethylene in methylene chloride was determined to be 0.18 mol/L·atm in ref 8.

(30) Popeney, C. S.; Guan, Z. *J. Am. Chem. Soc.* **2009**, *131*, 12384–12393.

(31) It is interesting to note that the kinetic preference of sandwich **s-2b** for trapping vinyl trialkoxysilane relative to ethylene is 10 times greater the thermodynamic preference of the less bulky traditional **t-1b** for binding vinyl trialkoxysilane versus ethylene. One possible explanation for this unexpected difference is that the transition state for displacement of ether in the kinetic experiment comes early and does not experience the degree of steric crowding that is felt when olefins are fully bound.

(32) The β -agostic alkyl intermediates are initially formed from the insertion of ethylene into the $\text{Pd}(\text{alkyl})(\text{C}_2\text{H}_4)$ complex under the polymerization.

(33) It is likely relative trapping rates are smaller when palladium complexes bearing an alkyl chain substituent larger (i.e., $\text{Pd}(\text{alkyl})$) than methyl (i.e., $\text{Pd}(\text{CH}_3)$) are trapped.